Induction of immunogenic cell death in cancer cells by a photoactivated platinum(IV) prodrug

Vojtech Novohradsky,[a] Jitka Pracharova, [a,b] Jana Kasparkova, [a] Cinzia Imberti,[c] Hannah E. Bridgewater,[c] Peter J. Sadler [c] and Viktor Brabec [a]

a) Czech Academy of Sciences, Institute of Biophysics, Kralovopolska 135, CZ-61265 Brno, Czech Republic.
b) Department of Biophysics, Centre of the Region Hana for Biotechnological and Agricultural Research, Palacky University, Slechtitelu 27, 783 71 Olomouc, Czech Republic
c) Department of Chemistry, University of Warwick, Coventry CV4 7AL, UK

Abstract

The platinum(IV) prodrug trans,trans,trans-[$Pt(N_3)_2(OH)_2(py)_2$] (1) is stable and non-toxic in the dark, but potently cytotoxic to cancer cells when irradiated by visible light, including cisplatin-resistant cells. On irradiation with visible light, it generates reactive Pt(II) species which can attack DNA, and produces reactive oxygen species (ROS) and reactive nitrogen species (RNS) which exert unusual effects on biochemical pathways. We now show that its novel mechanism of action includes induction of immunogenic cell death (ICD). Treatment of cancer cells with 1 followed by photoirradiation with visible light induces calreticulin (CRT) expression at the surface of dying cancer cells. This is accompanied by release of high mobility group protein-1B (HMGB1) and the secretion of ATP. Autophagy appears to play a key role in this chemotherapeutically-stimulated ICD. The observed uneven distribution of ecto-CRT promotes phagocytosis, confirmed by the observation of engulfment of photoirradiated CT26 colorectal cancer cells treated with 1 by J774.A1 macrophages. The photoactivatable prodrug 1 has a unique mechanism of action which distinguishes it from other platinum drugs due to its immunomodulating properties, which may enhance its anticancer efficacy.

Introduction

Platinum complexes represent a widely used class of anticancer drugs.[1] Some of these agents, e.g., cisplatin and its derivatives (carboplatin and oxaliplatin), belong to an important group of clinical cytostatics which are very successful both medicinally and commercially. Their clinical use is, however, limited due to undesirable side effects and a relatively narrow spectrum of sensitive tumors. These drawbacks provide an impetus for the search and design of new, more effective antitumor platinum complexes, which might overcome the limitations connected with the clinical use of conventional platinum cytostatics.

For cisplatin and carboplatin, it is generally accepted that nuclear DNA is the major pharmacological target of their anti- tumor action.[1,2] In other words, their antitumor effects are a consequence of their capability of damaging DNA in a unique way and the subsequent processing of this damage by cellular components.[3–5] A very large number of new antitumor platinum complexes have been tested, including agents whose mechanism of action (MoA) has been associated with an ability to damage DNA similar to cisplatin, but also some have a different MoA or a combination of various MoAs. The development of photoactivatable platinum(IV) complexes is a new strategy for design of antitumor platinum complexes which would act by an MoA different from that of cisplatin and its direct derivatives.[6,7] A promising complex in this class of photoactivatable platinum antitumor prodrugs is trans,trans, trans-[$Pt(N_3)_2(OH)_2(py)_2$] (1) (Fig. 1).[8–10]

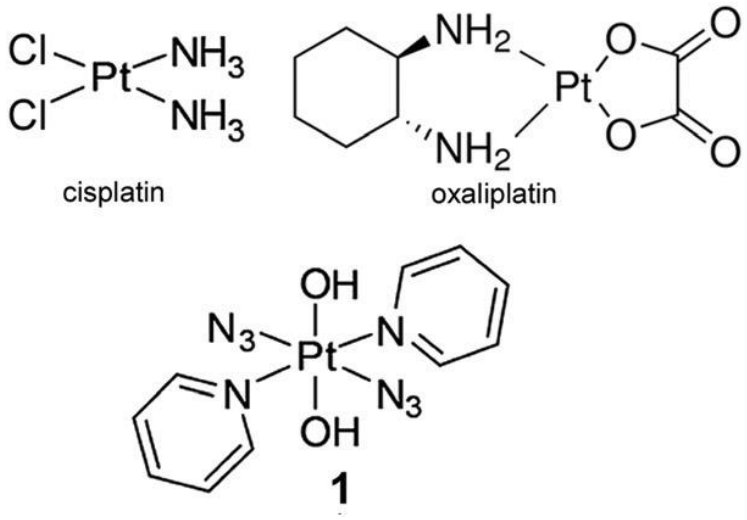

Figure 1. The structures of cisplatin, oxaliplatin, and complex 1.

This Pt^{IV} diazido complex is unreactive in the dark, but potently cytotoxic when photoactivated by UVA and visible light even in cisplatin-resistant tumor cell lines, with a high phototoxicity index. With regard to its MoA, the octahedral Pt^{IV} prodrug 1 is reduced upon photoactivation to square planar Pt^{II} species, which bind strongly to nuclear DNA and are toxic to tumor cells.[11,12] Notably, DNA damage by photoactivated 1 produces several downstream cellular effects different from those triggered in cancer cells by cisplatin-damaged DNA. Moreover, photo-reduction of 1 results in the release not only of Pt^{II} species, but also of other photo-products including azidyl and hydroxyl radicals, nitrenes, and singlet oxygen.[8,9] These photoreduction products can modulate biochemical pathways in tumor cells which are not involved in the MoA of cisplatin and its direct derivatives, thus pointing to a novel MoA for 1.[9]

One possibility of how the photoreduction products of 1 might act by an MoA different from that involving DNA damage (and typical for cisplatin and its direct derivatives) is that irradiated 1 could induce an immunogenic form of cell death (ICD). This suggestion is corroborated by convincing evidence demonstrating that some conventional antitumor metallodrugs (including oxaliplatin and its analogs[13–17]) can also induce ICD that synergistically enhances their anticancer efficiency, confirming the immunomodulating capability of chemotherapy. It has also been shown[15,18–20] that ICD-associated immunogenicity can be evoked through reactive oxygen species (ROS). Thus, it was reasonable to assume that the photoactivated 1, which generates ROS and RNS,[8,9] could induce, besides apoptosis, also ICD. Therefore, we investigated whether photoactivated 1 can induce ICD in vitro, which could synergistically enhance its anticancer efficiency, thus corroborating the immunomodulating capability of chemotherapy based on this photoactivatable Pt^{IV} prodrug.

Results and discussion

ICD is characterized by a series of biochemical hallmarks including: (i) translocation of ER-resident calreticulin (endo-CRT) to the cell surface (ecto-CRT) during early apoptosis; (ii) active secretion of ATP; (iii) extracellular secretion of nuclear high-mobility group box 1 protein (HMGB1) at late-stage apoptosis.[21] Additionally, a critical step for ICD is the engulfment of dying cancer cells by dendritic cells,[22] so the ICD inducers should also increase tumor cell phagocytosis.[16] Therefore, to determine whether photoactivated 1 can be identified

as an immuno-chemotherapeutic agent, we examined its capability of displaying the aforementioned characteristic hallmarks of ICD.

Irradiated 1 induces calreticulin exposure

Under the physiological (non-stress) conditions, CRT is usually located in the lumen of the endoplasmic reticulum (ER). CRT is translocated to the cell membrane during ICD stimulation (termed ecto-CRT). Thus, immunogenic chemotherapy induces CRT exposure at the cell surface of dying cells, which acts as the dominant pro-phagocytic signal promoting the engulfment of cancer cells.[22,23]

Human A2780 ovarian cancer cells were treated with increasing concentrations of 1 in the dark or under irradiation conditions [420 nm (blue light), 77 W m^{-2}, 30 min] for 2 h. The cells were subsequently washed and incubated for another 22 h in drug-free medium (for details, see the Experimental section in the ESI†) to stimulate an adequate cellular response. In these experiments, the anthracycline antimetabolite doxorubicin[22] and oxaliplatin[13] were used for comparative purposes as positive controls, whereas cisplatin[24] served as the negative control. The samples were fixed by 4% formaldehyde, stained with antiCRT-alexa fluor 488 conjugate, and counterstained with propidium iodide. These samples were further analyzed using flow-cytometry. Propidium iodide-negative cells were gated out to eliminate possible false-positive results due to the non-specific accumulation of anti-CRT antibody through the compromised cell membranes of dying cells (Fig. 2). Data were analyzed in terms of the overall mean fluorescence (mean fluorescence intensity; MFI) (Fig. 2B) and percent of the propidium iodide negative/CRT positive population (Fig. 2C). The histograms for irradiated samples are shown in Fig. 2A, whereas histograms obtained for samples kept in the dark are shown in ESI Fig. S1.†

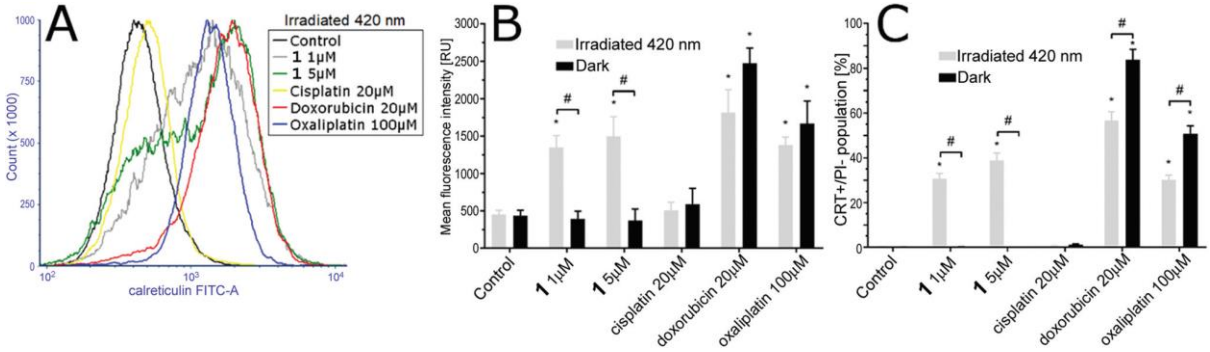

Figure 2. Analysis of ecto-CRT exposure after the treatment of A2780 cells with the investigated compounds. A2780 cells were untreated or treated with the indicated concentration of the tested compound for 2 h in the dark, or under irradiation conditions [90 min pre-incubation followed by irradiation with blue light (420 nm, 77 W m−2, 30 min)]; the samples were subsequently incubated for 22 h in the drug-free medium, and then analyzed by flow cytometry. A. Representative histograms from five independent experiments. B. Samples analyzed for overall mean fluorescence. C. Samples analyzed as the CRT-positive/PI-negative population. Stars (*) and hashes (#) at the top of the bars in both Fig. 2B and C indicate statistically significant difference from the untreated control ($p \leq 0.01$) and statistically significant difference between irradiated and nonirradiated samples ($p \leq 0.01$), respectively. Three independent experiments were done in quadruplicate for each sample set and the data in Fig. 2B and C show the mean ± SD.

The amount of immuno-detectable ecto-CRT observed on the surface of non-treated A2780 cells in the dark and under irradiation conditions was very small. Unsurprisingly, when cisplatin (20 μM), incapable of inducing ICD, was added to A2780 cells both in the dark or

under irradiation conditions, the induction of ecto-CRT exposure remained low, comparable with that observed for the untreated cells. In contrast, wellknown ICD inducers doxorubicin (20 μM) and oxaliplatin (100 μM) caused a relatively extensive induction of ecto-CRT exposure both in the dark and under irradiation conditions (Fig. 2B and C). Importantly, 1 (1 or 5 μM) induced ecto-CRT exposure extensively under irradiation conditions, but it was ineffective in the dark.

As another means of exploring the efficiency of 1 to induce ecto-CRT exposure, we investigated ecto-CRT exposure by confocal microscopy (Fig. 3). A2780 cells were treated with 1 and kept in the dark or under the irradiation conditions (*vide supra*). Then, the cells were fixed with 4% formaldehyde under non-permeabilizing conditions and stained with the anti-CRTalexa fluor 488 conjugate. Samples were visualized by confocal microscopy. It is shown in Fig. 3 that the fluorescence signal yielded by the cells stained by anti-CRT-alexa fluor 488 antibodies is localized on the cell membrane of the cells treated with 1, but only when the cells treated with 1 were irradiated. Qualitatively identical results were obtained when the cells were treated with doxorubicin and oxaliplatin (ESI Fig. S2†). In contrast, the untreated cells or cells treated with the 1 in the dark or with cisplatin yielded no fluorescence signal indicating lack of calreticulin exposure.

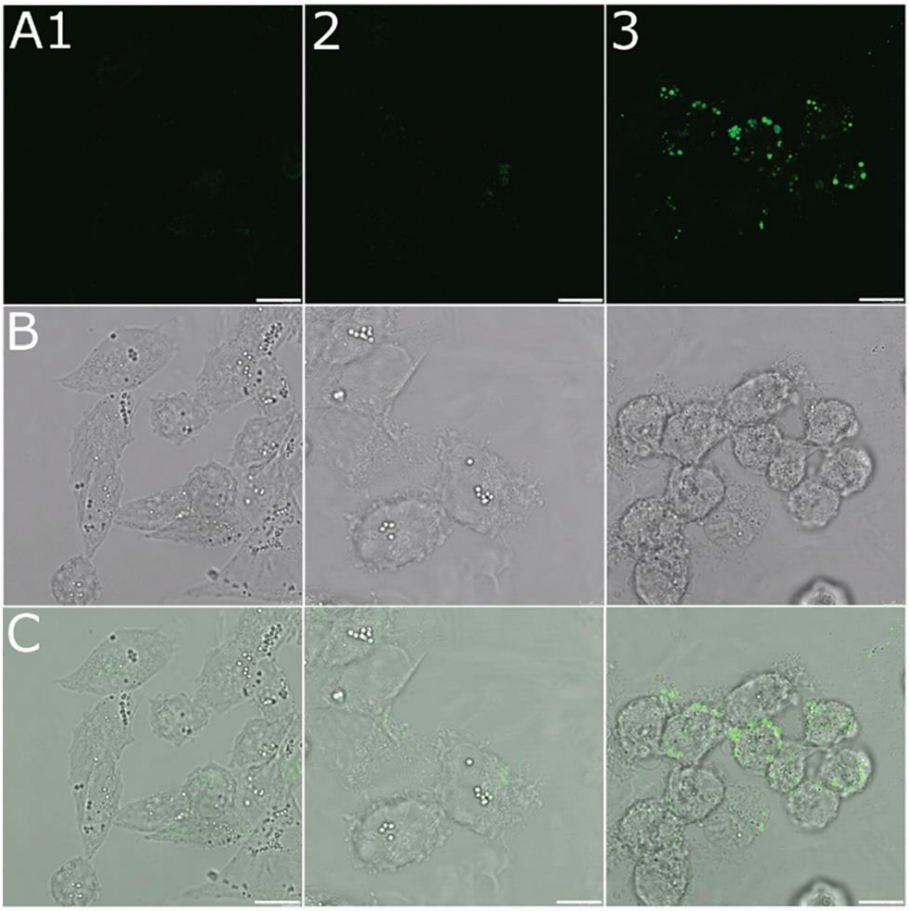

Figure 3. Immunofluorescence analysis of ecto-CRT exposure by confocal microscopy. A2780 cells were untreated or treated with 1 (5 μM) for 2 h in the dark (panels 1 and 2, respectively) or under irradiation conditions [90 min pre-incubation followed by irradiation with blue light (420 nm, 77 W m−2, 30 min)] (panel 3); the samples were subsequently incubated for 22 h in the drug-free medium. Channels: A. Fluorescence signal from CRT-Alexa fluor 488 conjugate. B. Bright field. C. Merge of the fluorescence and bright field channels. Scale bars represent 10 μm.

The results of analysis by confocal microscopy of A2780 cells treated with photoactivated 1 showed an uneven distribution of ecto-CRT on the surface of the cells Fig. 3C. This phenomenon was also observed for other ICD inducers and was proposed to promote phagocytosis.[25,26] Collectively, the results of the confocal microscopic experiments are consistent with the conclusions drawn[13,26,27] on the basis of flow cytometric analysis (Fig. 2) demonstrating that photoactivated 1 promotes surface exposure of calreticulin (ecto-CRT) which has emerged as a key mediator of the immunogenicity of dying tumor cells.22

Release of the high mobility group box 1 protein (HMGB1) and ATP to the extracellular environment.

In response to immunogenic chemotherapeutics, dying cells release HMGB1 protein, and secrete ATP into the extracellular environment after permeabilization of nuclear and cytoplasmic membranes, stimulating an immunogenic response. Moreover, neutralization or depletion of HMGB1 leads to the loss of the immunogenicity of cell death.[28] Thus, the release of the nuclear HMGB1 and ATP secretion to extracellular milieu determines, together with the induction of ecto-CRT exposure, the immunogenicity of dying tumor cells.[29–31] It is also important to mention that ecto-CRT exposure, HMGB1 release, and ATP secretion are all indispensable for ICD, i.e., that the absence of even one of these ICD hallmarks abolishes the efficacy of immunochemotherapy.[15,31]

To verify whether HMGB1 release and ATP secretion play a role in the mechanism of action of photoactivated 1, we analyzed stimulation of HMGB1 release and ATP secretion in the cell culture supernatants of A2780 cells incubated in the dark and under irradiation conditions with 1, and for comparative purposes also doxorubicin, oxaliplatin, and cisplatin. HMGB1 release was detected by the enzyme-linked immunosorbent assay (ELISA), and the extracellular ATP from cell supernatants was analyzed with the ATP bioluminescence assay kit CLSII (Roche).

Photoactivated (irradiated by visible light) 1 along with doxorubicin and oxaliplatin (both in the dark) induced the marked release of HMGB1 and ATP from the nuclei of ovarian A2780 cancer cells in a concentration-dependent manner (Fig. 4 and 5, respectively). In contrast, no or very low extracellular release of nuclear HMGB1 and ATP was detected if the A2780 cells were untreated or treated with 1 and cisplatin in the dark. Altogether, these results corroborate the importance of HMGB1 and ATP release into the extracellular environment for the immune response against tumor cells dying in response to photoactivated 1. Notably, when doxorubicin or oxaliplatin was added to A2780 cells under irradiation conditions, the release of HMGB1 and ATP secretion decreased considerably as compared to that found for the treatment with doxorubicin or oxaliplatin in the dark (Fig. 4). Similarly, the induction of ecto-CRT exposure considerably decreased after doxorubicin or oxaliplatin was added to A2780 cells under irradiation conditions as compared to that found for the treatment with doxorubicin or oxaliplatin in the dark (Fig. 2). It is, therefore, possible to expect that the combination of doxorubicin or oxaliplatin chemotherapy with photodynamic therapy by other agents might decrease the chemotherapeutic effects of these two drugs or alter their ability to induce ICD.

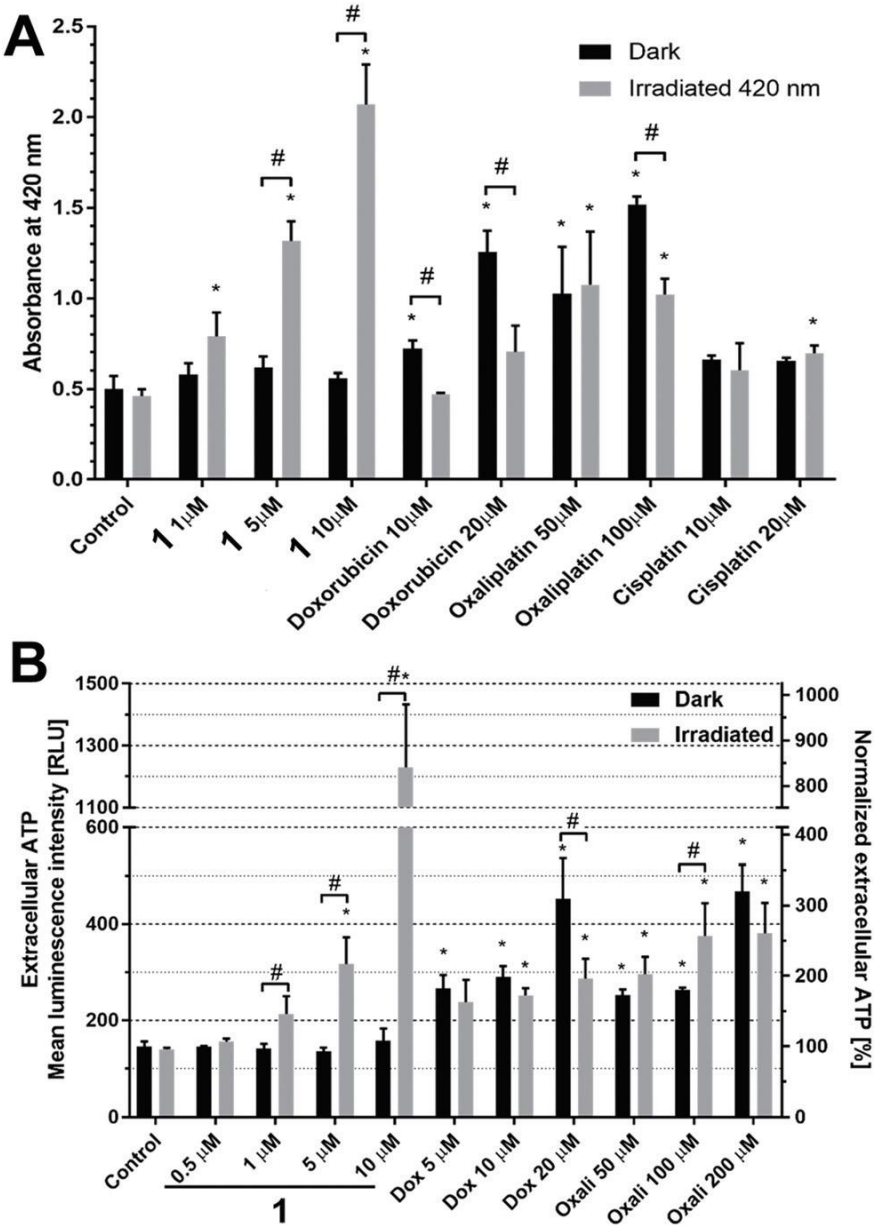

Figure 4. Extracellular release of (A) HMGB1, and (B) ATP. A. A2780 cells were untreated or treated with the indicated concentrations of the tested compound for 2 h in the dark or under irradiation conditions [90 min pre-incubation followed by irradiation with blue light (420 nm, 77 W m−2, 30 min). The samples were subsequently incubated for 22 h in the drug-free medium, and then analyzed by the ELISA assay. The results are expressed as the absorbance at 420 nm corresponding to the product yielded by the ELISA enzyme, which is proportional to the amount of HMGB1 protein released from the cells. B. A2780 cells were treated with the indicated concentrations of the tested compounds as described for panel A. The samples were analyzed by the ATP bioluminescence assay. Data are expressed as the mean luminescence intensity [RLU] or normalized to untreated non-irradiated control samples expressed in percentages. Stars (*) and hashes (#) at the top of the bars in both Fig. 4A and B indicate statistically significant difference from the untreated control ($p \leq 0.01$) and statistically significant difference between irradiated and non-irradiated samples ($p \leq 0.01$), respectively. Three independent experiments were done in quadruplicate for each sample set and the data in Fig. 4a and B show the mean ± SD.

Involvement of autophagy in ICD-associated ATP secretion

Autophagy plays a crucial role in ATP secretion during chemotherapeutically stimulated ICD.[32] This conclusion is also corroborated by the observation that autophagy-deficient cells are unable to trigger tumor-targeting immune responses.[33] Additionally, the autophagy-deficient tumors growing in immunocompetent hosts are generally less sensitive to anti-cancer agents that actively promote a therapeutically relevant immune response like doxorubicin and oxaliplatin.[34,35] Moreover, functional autophagy machinery is required for survival of the cells involved in adaptive anticancer immunity, like cytotoxic T-lymphocytes.[36] Activating autophagy in treated tumors may boost the overall efficacy of anticancer therapy, mainly in terms of ICD.[37]

Since autophagy can play an essential role in the immunogenic release of ATP from dying cells, we examined the relationship between extracellular ATP release driven by the autophagy machinery and cell death by means of multi-parameter flow cytometry. We analyzed three main modes of cell death (apoptosis, necrosis, and autophagy) initiated after the treatment of ovarian cancer cells A2780 with 1. All three main modes of cell death were analyzed directly in one experiment, to compare the direct contribution of each mode on the overall death of the treated cells.

A2780 cells were treated with 1 in the dark and under irradiation conditions, and apoptotic, necrotic, and autophagic mechanisms of cell death were measured by flow cytometry. The results were compared with the effects of the established specific cell-death inducers, namely staurosporine, a known inhibitor of protein kinases, for specific induction of apoptosis, which was detected by annexin-V, EtOH, a known stimulator of non-specific necrosis, which was detected by propidium iodide, a combination of rapamycin and chloroquine, known stimulators of autophagy, which was detected with a Cyto-ID probe (rapamycin stimulates the accumulation of autophagic vacuoles and the autophagic flux, whereas chloroquine increases lysosomal pH, thereby inhibiting lysosomal activity during autophagosome-lysosome fusion[38]). As a result, this combinatorial treatment provides more autophagy-positive cells than single-agent treatment.

Cells treated with 1 in the dark displayed only very small changes over the untreated control in the distribution among the investigated types of cell death (Fig. 5). In contrast, photoactivated (irradiated by visible light) 1 induced cell death mainly via autophagic and, to a lesser extent, via apoptotic pathways (Fig. 5). Thus, these results support the view, and are consistent with, the hypothesis that autophagy is essential for the immunogenic release of ATP from dying cells when A2780 cells are treated with photoactivated 1.

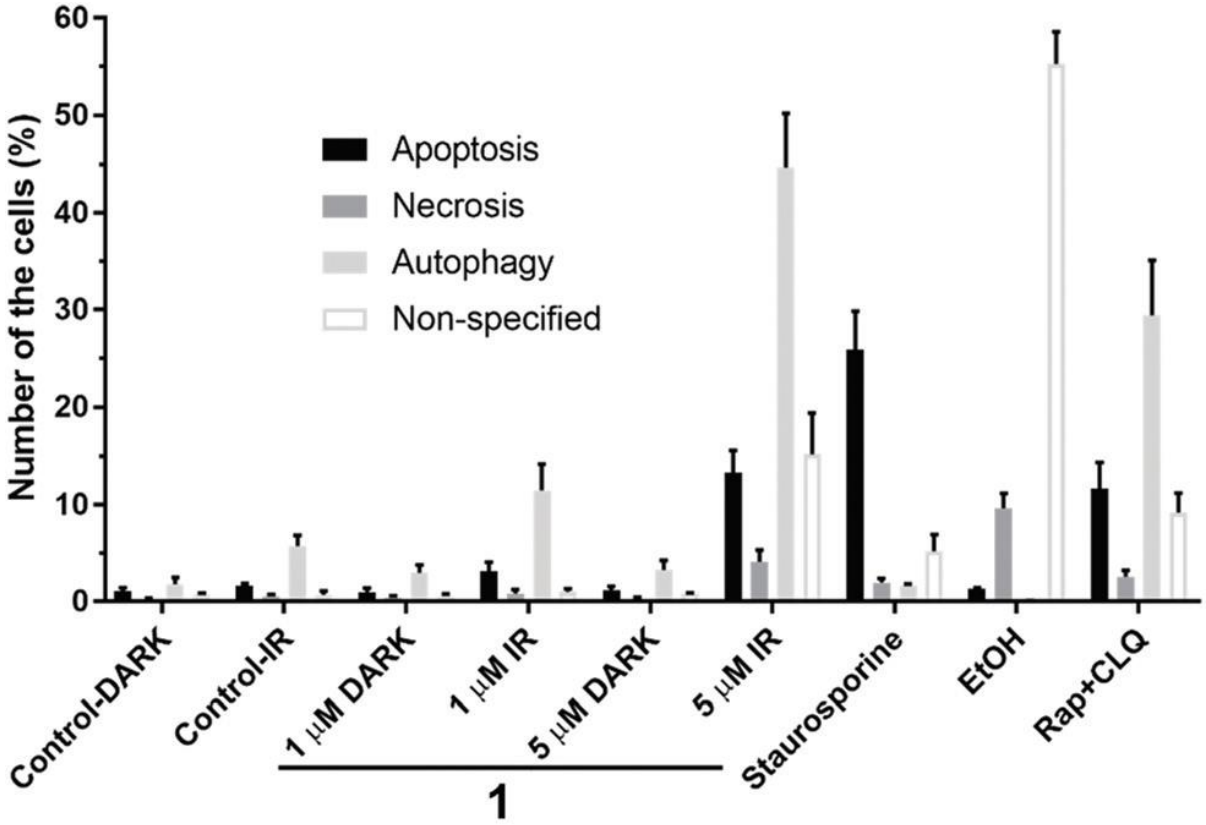

Figure 5. Analysis of the mode of cell death. A2780 cells were treated with 1 or 5 μM of 1 for 90 min; then, the samples were further incubated for an additional 30 min in the dark or under irradiation conditions (blue light 420 nm, 77 W m−2). Fluorescence signals yielded by the specific probes for apoptosis (annexin-V), necrosis (propidium iodide), and autophagy (Cyto-ID) were analyzed by flow cytometry. The cells were also treated with staurosporine (positive control for apoptosis) (1 μM, 3 h), EtOH (positive control for necrosis) [10% (v/v), 90 min] and rapamycin with chloroquine (positive control for autophagy) (0.5 and 50 μM, 18 h). The results are expressed as the mean number of the cells (%) positive for the specific cell death probe. Three independent experiments were done in quadruplicate for each sample set.

In vitro phagocytosis assay

Besides the externalization of ecto-CRT, the release of HMGB1 and secretion of ATP, also efficient phagocytic removal by professional phagocytes belong to the most important biochemical hallmarks of ICD.[39] Additionally, phagocytosis was shown to be mediated by cell surface exposure of ecto-CRT. On the other hand, it has been also demonstrated that translocation of CRT to the cell surface is necessary, but not sufficient for the induction of phagocytosis. The clinically used platinum(II) antitumor drug oxaliplatin has been presented as a compound capable of effective externalization of ecto-CRT and induction of ICD,[13] but also being unable to promote phagocytosis.[26] Therefore, we evaluated in an in vitro phagocytosis assay to determine whether photoactivated 1 can increase tumor cell phagocytosis over non-treated controls or 1 in the dark.

To do this, murine CT26 carcinoma cells (colon fibroblasts), used as a model for studies on the immune response, were untreated or treated with 1 in the dark or under irradiation conditions as described in the Experimental section and coincubated with murine J774.A1 macrophages. CT26 cells and J774.A1 macrophages were pre-stained with CellTrackerTM

green CMFDA and CellTrackerTM red CMTPX, respectively, and analyzed by flow cytometry (Fig. 6A–C and S3†) and confocal microscopy (Fig. 6D and E). Representative flow cytometry density plots showing phagocytosis (top right quadrant) with 1 in the dark and irradiated 1 (both at 10 μM concentration) are shown in Fig. 6B and C, respectively.

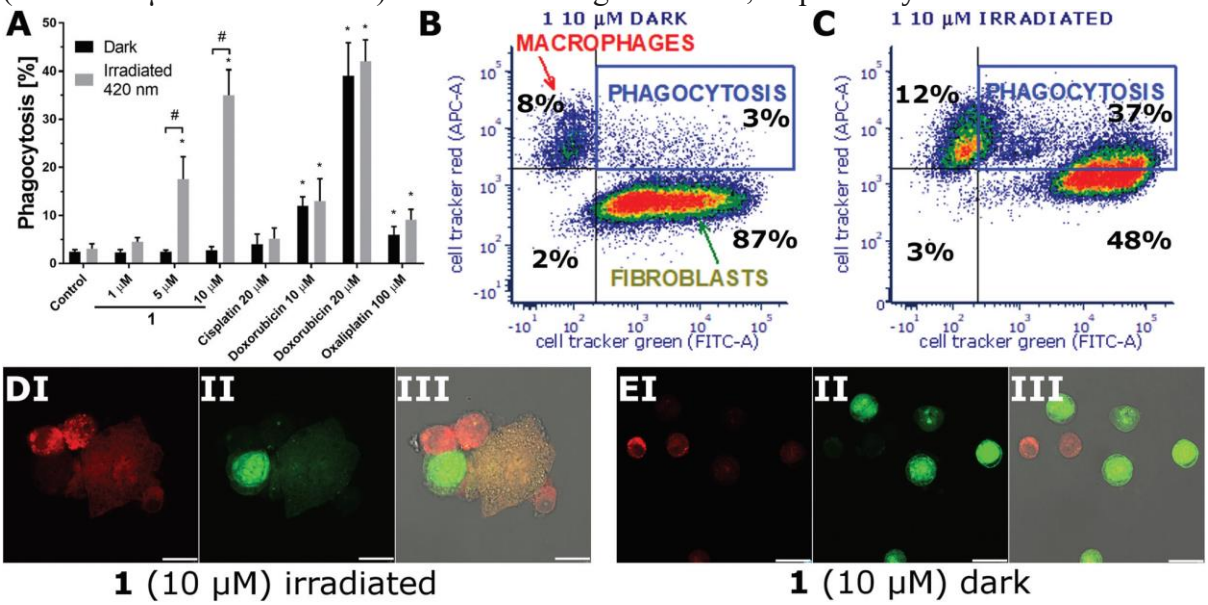

Figure 6. In vitro phagocytosis assay. Green-stained murine CT26 carcinoma cells were treated with the investigated compounds at the indicated concentrations for 24 h and subsequently co-incubated with red-stained J774.A1 murine macrophages for 3 h. A. Analysis of phagocytosis in CT26 cells by flow cytometry. The percentage of phagocytosis was calculated from the number of double-stained macrophages compared to the total number of macrophages. B and C. Representative flow cytometry density plots showing the phagocytosis after the treatment with 1 (10 μM) in the dark (B) or upon irradiation (C). D and E. Confocal microscopy of J774.A1 macrophages (red) engulfing CT26 cells (green) is evident by mixing of the dyes. The symbols I, II, and III in the panels D and E indicate the red-stained J774.A1 macrophages, the green-stained CT26 fibroblasts, and the overlay of the red, green and bright field channels, respectively. Scale bars in panels D and E represent 30 or 60 μm, respectively.

Photoactivation of 1 markedly increased tumor-cell phagocytosis compared with 1 in the dark or non-treated controls (35.1 ± 5.6% vs. 2.8 ± 0.4% or 2.4 ± 0.2%, respectively, $p < 0.001$) (see also Fig. 6A). Other representative flow cytometry density plots showing phagocytosis with doxorubicin, cisplatin, and oxaliplatin are shown in the ESI Fig. S3.† Except for doxorubicin (20 μM, a well-known inducer of ICD and phagocytosis[40]), the other investigated compounds, cisplatin (20 μM, incapable of inducing ICD[16]) and oxaliplatin (100 μM, classical ICD inducer[13,41]) promoted phagocytosis only negligibly irrespective of dark or irradiated conditions (Fig. 6A). Collectively, our results indicate that the photoactivation of 1 markedly promotes tumor cell phagocytosis and also confirm that although oxaliplatin induces ICD and key pro-phagocytic signal ecto-CRT exposure,[42] it does not promote tumor cell phagocytosis.[26]

Phagocytosis induced by photoactivated 1 was also verified by confocal microscopy (Fig. 6D), which showed the contact of red-colored murine J774.A1 macrophages with green-colored murine CT26 carcinoma cells. Moreover, analysis by confocal microscopy also revealed engulfment of CT26 cells by J774. A1 macrophages, demonstrated in Fig. 6D-III by mixing of the fluorescent red and green dyes in the area of the engulfment. The control experiments performed with cells treated with 1 in the dark showed that both co-incubated C26

and J774.A1 cells were well separated without mixing of the fluorescent red and green dyes (Fig. 6E). Thus, the results of the confocal microscopic analysis are entirely consistent with the analysis by flow cytometry, confirming the ICD-stimulatory effect of 1 when photoactivated with visible light.

In summary, this report demonstrates a new mechanism of antitumor action of trans,trans,trans-[$Pt(N_3)_2(OH)_2(py)_2$] (1), a photoactivatable Pt^{IV}-based chemotherapeutic agent, which besides DNA damage[12] also involves synergistic action through induction of an immunogenic form of cell death (ICD). This prodrug, when photoactivated by visible light, was found to display the characteristic hallmarks of ICD inducers, namely calreticulin exposure, HMGB1 and ATP release in ovarian carcinoma cells, and promotion of tumor cell phagocytosis in model murine (colon fibroblasts) carcinoma cells. Additionally, autophagy was found to be essential for the immunogenic release of ATP from dying tumor cells which had been treated with the Pt^{IV} prodrug and photoirradiated.

It seems likely that the molecular mechanism of the ICD induced by photoactivated 1 involves oxidative attack on proteins (e.g. on Met and Trp residues) by the ROS and RNS, and perhaps also by the Pt^{II} species, it generates.[7,43] In particular photoactivated 1 induces oxidation of Met, Trp and the Cys residues in the catalytic center of the enzyme thioredoxin reductase (TrxR), which protects cells against ROS, resulting in inhibition of TrxR activity and further ROS damage.[44] Therefore it is possible that 1 acts as a type II ICD inducer, with ROS directly triggering ER stress, resulting in exposure of calreticulin.[41] That the generated ROS could damage the ER was confirmed by confocal microscopy (Fig. S4†). The results of this experiment show that after the cells treated with 1 were irradiated, the ROS were produced in the whole cytoplasm, including the ER. This type of ICD induction is rarer than type I (indirect activation of ER stress) which has previously been observed for oxaliplatin, but has been reported for some other agents including a cyclometallated Pt^{II} complex which targets the ER.[26]

Clinical application of photochemotherapy is currently based on photosensitizers for photodynamic therapy, which typically need oxygen to exert their anticancer action. As many malignant and most aggressive tumors are of oxygen-deficient nature,[45] the requirement for oxygen is a major drawback of these phototherapeutic agents. In contrast, the investigated platinum(IV) prodrug 1 does not require the presence of oxygen for its anticancer effects, as these stem from chemical photodecomposition of 1 to release cytotoxic species.[9] Accordingly, 1 presents a potential key advantage over PDT photosensitizers. Thus, this photocytotoxic Pt^{IV} complex was identified as the first platinum immuno-chemotherapeutic agent suitable for photochemotherapy also in the hypoxic milieu of tumors.

It might be argued that 1 is photoactivated by irradiation with light of a relatively short wavelength (420 nm). This fact might be a limitation for the clinical application of this diazidoplatinum(IV) complex since the light of such high energetic wavelengths can poorly penetrate some solid tumors. However, the current level of laser and fiber-optic methodologies allows also irradiating internal organs with light of defined wavelength, including blue light.[6] On the other hand, the capability of longer-wavelength light, which penetrates deeply into tumor tissue might, in some cases also be a drawback of photodynamic therapy. The choice of the optimal wavelength range also depends on the depth of tumor invasion; unnecessary deeper tissue penetration may also impair the potency of photodynamic therapy and damage underlying healthy tissues.[46]

Experimental

Chemicals

Trans,trans,trans-[$Pt(N_3)_2(OH)_2(py)_2$] (1) was synthesized and characterized by the method described previously.[11] Oxaliplatin, doxorubicin, staurosporine, rapamycin, chloroquine were from Merck (Germany). Ovarian carcinoma A2780 cells were kindly supplied by Professor B. Keppler from the University of Vienna (Austria). Murine (colon fibroblasts) CT26 carcinoma cells and murine J774.A1 macrophages were from ECACC (UK). 3-(4,5-Dimethyl-2-thiazolyl)-2,5-diphenyl-2Htetrazolium bromide (MTT) was from Calbiochem (Darmstadt, Germany).

Cell treatment schedule and irradiation

The cells were incubated with the relevant agent for a total of 2 h in the dark or under irradiation conditions [420 nm (blue light), 77 W m^{-2}, for 30 min after 90 min incubation]. The cells were subsequently washed and incubated for another 22 h in the drug-free medium. A Luzchem photoreactor [LZC-ICH2 from Luzchem (Canada)] with temperature controller and with blue lamps [77 W m^{-2} (28 J cm^{-2}); λ_{max} = 420 nm] was used for irradiation. The medium in which the irradiation was performed consisted of Hank's Balanced Salt Solution HBSS without antibiotics or any additives. The temperature in the light chamber during irradiation was 37 °C. After the irradiation, cells were washed with HBSS, and samples were loaded with full culture medium containing antibiotics and FBS.

Antiproliferative activity

The antiproliferative activity of the investigated compounds was evaluated by using a system based on the tetrazolium compound MTT. The A2780 cells were seeded in 96-well tissue culture plates at a density of 1×10^4 cells per well in 100 μL of the medium. After overnight incubation (16 h) at 37 °C in a 5% CO_2 humidified atmosphere, the medium from the wells was removed, and cells were treated according to the procedure described in the preceding paragraph. After an additional 70 h incubation, 20 μL of MTT solution (1.25 mg mL^{-1} in PBS) was added to each well, and the plates were incubated for 4 h. At the end of the incubation period, the medium was removed and the formazan product was dissolved in 100 μL of DMSO. The cell viability was evaluated by measurement of the absorbance at 570 nm (reference 620 nm), using an Absorbance Reader (SPARK, Tecan). All experiments were made in triplicate. The readings were converted to the percentage of control (% cell survival). Antiproliferative effects were expressed as IC_{50} values calculated from curves constructed by plotting cell survival (%) versus drug concentration (μM) (IC_{50} = concentration of the agent inhibiting cell growth by 50%). Concentrations of Pt platinum compounds present in medium during the treatment were verified by FAAS.

Exposure of calreticulin

Two independent experimental methods were used to identify CRT exposure. The samples were quantitatively analyzed using flow cytometry, whereas the qualitative analysis was performed with the aid of confocal microscopy.

Detection of CRT exposure by flow cytometry. A2780 cells were seeded on the 6-well plate at the density of 2×10^5 cells per well and incubated overnight. Then the cells were treated with 1 (1 and 5 μM), doxorubicin (20 μM), oxaliplatin (100 μM) or cisplatin (20 μM), and then further incubated as described above. Subsequently, the cells were fixed with 4% formaldehyde and stained with antiCRT-alexa fluor 488 conjugate (Abcam). Before the analysis on a flow cytometer (BD FACSVerse), the cells were co-stained with propidium iodide. Single cells (3×10^4) were analyzed and plotted on the histogram with a bi-exponential scale. For population

analysis, acquired events were plotted on 2D density plots, and the CRTpositive population was identified in CRT+/PI-quadrant; the number of the cells was expressed in percentages from the single gated cells. Data were analyzed using FCS Express 6 (DeNovo software; Glendale, CA).

Detection of CRT exposure by confocal microscopy. A2780 cells were seeded on 50 mm glass-bottom culture dishes (Mattek, Ashland, USA) at a density of 2×10^5 cells per dish, and incubated overnight. Then the cells were treated with 1 (1 and 5 μM), doxorubicin (20 μM), oxaliplatin (100 μM) or cisplatin (20 μM) and the treatment continued as described above. Subsequently, the cells were fixed with 4% formaldehyde and stained with antiCRT-alexa fluor 488 conjugate (Abcam). Samples were visualized on a confocal microscope Leica TCS SP8 SMD (Leica microsystems GmbH, Wetzlar, Germany).

Release of the high mobility group box 1 protein (HMGB1) to the extracellular space

The release of the HMGB1 protein was assayed using the ELISA kit from IBL International (Tecan). A2780 cells were seeded on 96-well plates (TPP) at a density of 10 000 cells per well and incubated for 48 h. Then the cells were treated with the increasing concentrations of 1 (1, 5, 10 μM), doxorubicin (10, 20 μM), oxaliplatin (50, 100 μM), or cisplatin (10, 20 μM), and the treatment continued as described above. After the treatment period, supernatants from centrifuged samples were transferred into the 96-well plate provided by the manufacturer with the wells containing the immobilized HMGB1 protein. The experimental protocol for the ELISA assay described in the manufacturer instructions was used. At the end of the assay, the colorimetric product was analyzed on a SPARK (Tecan) reader. The absorbance measured at 420 nm was proportional to the amount of HMGB1 protein released from the cells.

Extracellular ATP analysis

Extracellular ATP released from A2780 cells was detected using an ATP bioluminescence assay kit CLSII (Roche). A2780 cells were seeded on the 96-well black plate (Corning) at the density of 10 000 cells per well and incubated overnight. Then, the cells were treated with increasing concentrations of 1 (0.5, 1, 5, 10 μM), doxorubicin (5, 10, 20 μM) or oxaliplatin (50, 100, 200 μM) for 90 min and incubated at 37 °C, 5% CO_2 in the dark. Subsequently, the cells were irradiated with blue light or incubated in the dark for another 30 min. Then, the samples were washed with HBSS and incubated for 22 h in drug-free medium. The cells were centrifuged (200 g, 5 min), and supernatants were analyzed by using an ATP bioluminescence assay kit CLSII according to the manufacturer's instructions. Luminescence was measured on a SPARK reader (Tecan). The results are expressed as the mean luminescence intensity, or normalized to the untreated, non-irradiated control.

Determination of the mode of cell death

Apoptotic, necrotic, and autophagic mechanisms of cell death were investigated by the flow cytometry. A2780 cells were seeded on the 6-well plate at the density of 2×10^5 cells per well and incubated overnight. The cells were further treated as described in the section "Treatment schedule and irradiation of the samples" with 1 at the concentration of 0, 5, or 10 μM for 1 h in Earle's Balanced Salt Solution (EBSS). Staurosporine, ethanol, and chloroquine with rapamycin were used as the positive controls for apoptosis, necrosis, and autophagy, respectively. The cells were treated with 1 μM staurosporine for 3 h, while ethanol was added at 10% v/v for 90 min. Chloroquine was added at the final concentration of 50 μM together with 500 nM of rapamycin for 18 h in the culture media at 37 °C, 5% CO_2. The cells were harvested with CellStriper (Corning) at the end of the incubation period, pelleted, subsequently stained with CYTO-ID® autophagy detection probe, and incubated for another 30 min in the

culture medium without phenol red in a humidified CO_2 incubator. Then, the cells were centrifuged for 3 min at 300 g and stained with propidium iodide and annexin-V for 15 min at 25 °C. Samples were subsequently analyzed on a flow cytometer (BD FACSVerse). Data were analyzed using FCS Express 6 (DeNovo software; Glendale, CA).

In vitro phagocytosis assay

J774.A1 murine macrophages were seeded in a 75 cm^2 flasks at the density of 2×10^6 cells and incubated for 48 h. Murine CT26 cells were seeded in 6-well plate at the density of 1.5×10^5 cells per well and incubated overnight. The cells were further treated as described in the section "Treatment schedule and irradiation of the samples". Then, both cell lines were stained by cell trackers. J774.A1 macrophages were stained with CellTracker™ red CMTPX, and CT26 fibroblasts were stained with CellTracker™ green CMFDA, both from Invitrogen. The cells were co-incubated at the 1 : 5 macrophage : fibroblast ratio for 3 h, harvested, and fixed for 10 min with 4% formaldehyde. Phagocytosis was evaluated using flow cytometry (BD FACSVerse), and data were analyzed with the aid of FCS Express 6 (DeNovo software; Glendale, CA). Samples were also analyzed by confocal microscope using a Leica TCS SP8 SMD (Leica microsystems GmbH, Wetzlar, Germany).

Localization of ROS in A2780 cells

A2780 cells were seeded on confocal 35 mm glass bottom dishes (Mattek, Ashland, USA) at a density of 1.5×10^5 cells per dish and cultured overnight. Then, the cells were treated with 1 at a concentration of 5 μM or supplemented with fresh culture medium. Cells were incubated for 90 min under dark conditions followed by 30 min of irradiation with blue light (420 nm; 77 W m^{-2}). A set of samples were also incubated under dark conditions after the treatment. Then the cells were subsequently stained with ER tracker and CellROX reagent, washed twice with PBS and fixed with 4% formaldehyde for 15 min at room temperature. Cells were visualized on a confocal microscope Leica TSC SP8 SMD.

Statistical analysis

If not otherwise stated, the same symbols were used throughout the study to highlight statistically significant differences. Stars (*) at the top of the bars indicate a significant difference from the untreated control. Statistical difference between the irradiated and non-irradiated samples is marked with the hash (#). Statistical significance was calculated using the two-way analysis of variance (ANOVA) and unpaired Student's t-test with $p \leq 0.01$.

Conclusions

The results of our work might have broad implications for photoactivated chemotherapy of cancer owing to the current extensive use of platinum-based drugs in cancer treatment. Strategies based on simultaneous induction of ICD and DNA damage by platinum drugs upon light irradiation may result in efficient antitumor activity, taking advantage of the selective and targeted activation in tumor cells.

Collectively, our results warrant further investigation into the use of Pt^{IV}-based diazido compounds in photoactivated chemotherapy for the treatment of human tumors. They also highlight the importance of photoactivatable platinum complexes for synergistic enhancement of their anticancer efficiency due to their immunomodulating capacity.

Author contributions

V. N. and J. P. contributed equally to this work. The manuscript was written through contributions of all authors. All authors have given approval to the final version of the manuscript.

Conflicts of interest

There are no conflicts to declare.

Acknowledgements

This work was supported by the Czech Science Foundation (Grant 18-09502S), the Wellcome Trust (Grant 209173/Z/17/Z, Fellowship for C. I.), EPSRC (Grants EP/F034210/1 and EP/ P030572/1) and Anglo American Platinum Mike and Enfys Bagguley (PhD Studentship for H. E. B).

References

1. T. C. Johnstone, K. Suntharalingam and S. J. Lippard, The next generation of platinum drugs: Targeted Pt(II) agents, nanoparticle delivery, and Pt(IV) prodrugs, *Chem. Rev*., 2016, 116, 3436–3486.
2. V. Brabec, O. Hrabina and J. Kasparkova, Cytotoxic platinum coordination compounds. DNA binding agents, *Coord. Chem. Rev*., 2017, 351, 2–31.
3. D. Wang and S. J. Lippard, Cellular processing of platinum anticancer drugs, *Nat. Rev. Drug Discovery*, 2005, 4, 307–320.
4. Y. Jung and S. J. Lippard, Direct cellular responses to platinum-induced DNA damage, *Chem. Rev*., 2007, 107, 1387– 1407.
5. L. Kelland, The resurgence of platinum-based cancer chemotherapy, *Nat. Rev. Cancer*, 2007, 7, 573–584.
6. P. J. Bednarski, F. S. Mackay and P. J. Sadler, Photoactivatable platinum complexes, *Anti-Cancer Agents Med. Chem.,* 2007, 7, 75–93.
7. C. Imberti, P. Zhang, H. Huang and P. J. Sadler, New Designs for Phototherapeutic Transition Metal Complexes, *Angew. Chem*. *Int. Ed*, 2020, 59, 61–73.
8. Y. Zhao, N. J. Farrer, H. Li, J. S. Butler, R. J. McQuitty, A. Habtemariam, F. Wang and P. J. Sadler, De novo generation of singlet oxygen and ammine ligands by photoactivation of a platinum anticancer complex, *Angew. Chem., Int. Ed.*, 2013, 52, 13633–13637.
9. H. Y. Shi, C. Imberti and P. J. Sadler, Diazido platinum(IV) complexes for photoactivated anticancer chemotherapy, *Inorg. Chem. Front.,* 2019, 6, 1623–1638.
10. M. Pizarro, R. J. McQuitty, F. S. Mackay, Y. Zhao, J. A. Woods and P. J. Sadler, Cellular accumulation, lipophilicity and photocytotoxicity of diazido platinum(IV) anticancer complexes, *ChemMedChem*, 2014, 9, 1169–1175.
11. N. J. Farrer, J. A. Woods, L. Salassa, Y. Zhao, K. S. Robinson, G. J. Clarkson, F. S. Mackay and P. J. Sadler, A potent trans-diimine platinum anticancer complex photoactivated by visible light, *Angew. Chem., Int. Ed.*, 2010, 49, 1–5.
12. J. Pracharova, L. Zerzankova, J. Stepankova, O. Novakova, N. J. Farrer, P. J. Sadler, V. Brabec and J. Kasparkova, Interactions of DNA with a new platinum(IV) azide dipyridine complex activated by UVA and visible light: Relationship to toxicity in tumor cells, *Chem. Res. Toxicol.,* 2012, 25, 1099–1111.
13. A. Tesniere, F. Schlemmer, V. Boige, O. Kepp, I. Martins, F. Ghiringhelli, L. Aymeric, M. Michaud, L. Apetoh,L. Barault, J. Mendiboure, J. P. Pignon, V. Jooste, P. van Endert, M. Ducreux, L. Zitvogel, F. Piard and G. Kroemer, Immunogenic death of colon cancer cells treated with oxaliplatin, *Oncogene*, 2010, 29, 482–491.
14. U. Jungwirth, D. N. Xanthos, J. Gojo, A. K. Bytzek, W. Korner, P. Heffeter, S. A. Abramkin, M. A. Jakupec, C. G. Hartinger, U. Windberger, M. Galanski, B. K. Keppler and W. Berger, Anticancer activity of methyl-substituted oxaliplatin analog, *Mol. Pharmacol.,* 2012, 81, 719–728.

15. G. Kroemer, L. Galluzzi, O. Kepp and L. Zitvogel, Immunogenic cell death in cancer therapy, *Annu. Rev. Immunol.*, 2013, 31, 51–72.
16. A. Terenzi, C. Pirker, B. K. Keppler and W. Berger, Anticancer metal drugs and immunogenic cell death, *J. Inorg. Biochem*., 2016, 165, 71–79.
17. C. Rébé, L. Demontoux, T. Pilot and F. Ghiringhelli, Platinum derivatives effects on anticancer immune response, *Biomolecules*, 2019, 10, 13.
18. D. V. Krysko, A. D. Garg, A. Kaczmarek, O. Krysko, P. Agostinis and P. Vandenabeele, Immunogenic cell death and DAMPs in cancer therapy, *Nat. Rev. Cancer*, 2012, 12, 860–875.
19. O. Kepp, L. Menger, E. Vacchelli, C. Locher, S. Adjemian, T. Yamazaki, I. Martins, A. Q. Sukkurwala, M. Michaud, L. Senovilla, L. Galluzzi, G. Kroemer and L. Zitvogel, Crosstalk between ER stress and immunogenic cell death, *Cytokine Growth Factor Rev*., 2013, 24, 311–318.
20. W. Li, J. Yang, L. Luo, M. Jiang, B. Qin, H. Yin, C. Zhu, X. Yuan, J. Zhang, Z. Luo, Y. Du, Q. Li, Y. Lou, Y. Qiu and J. You, Targeting photodynamic and photothermal therapy to the endoplasmic reticulum enhances immunogenic cancer cell death, *Nat. Commun*., 2019, 10, 3349.
21. L. Menger, E. Vacchelli, S. Adjemian, I. Martins, Y. Ma, S. Shen, T. Yamazaki, A. Q. Sukkurwala, M. Michaud, F. Mignot, F. Schlemmer, E. Sulpice, C. Locher, X. Gidrol, F. Ghiringhelli, N. Modjtahedi, L. Galluzzi, F. André, L. Zitvogel, O. Kepp and G. Kroemer, Cardiac glycosides exert anticancer effects by inducing immunogenic cell death, *Sci. Transl. Med.*, 2012, 4, 143ra199.
22. M. Obeid, A. Tesniere, F. Ghiringhelli, G. M. Fimia, L.Apetoh, J.-L. Perfettini, M. Castedo, G. Mignot, T. Panaretakis, N. Casares, D. Métivier, N. Larochette, P. van Endert, F. Ciccosanti, M. Piacentini, L. Zitvogel and G. Kroemer, Calreticulin exposure dictates the immunogenicity of cancer cell death, *Nat. Med.*, 2007, 13, 54–61.
23. X. Liu, Y. Pu, K. Cron, L. Deng, J. Kline, W. A. Frazier, H. Xu, H. Peng, Y.-X. Fu and M. M. Xu, CD47 blockade triggers T cell–mediated destruction of immunogenic tumors, *Nat. Med.*, 2015, 21, 1209–1215.
24. Y. Xiang, L. Chen, L. Li and Y. Huang, Restoration and enhancement of immunogenic cell death of cisplatin by coadministration with digoxin and conjugation to HPMA copolymer, *ACS Appl. Mater. Interfaces*, 2020, 12, 1606– 1616.
25. S. J. Gardai, K. A. McPhillips, S. C. Frasch, W. J. Janssen, A. Starefeldt, J. E. Murphy-Ullrich, D. L. Bratton, P.-A. Oldenborg, M. Michalak and P. M. Henson, Cellsurface calreticulin initiates clearance of viable or apoptotic cells through trans-activation of LRP on the phagocyte, *Cell*, 2005, 123, 321–334.
26. Y. Q. Wong, W. W. F. Ong and W. H. Ang, Induction of immunogenic cell death by chemotherapeutic platinum complexes, *Angew. Chem., Int. Ed*., 2015, 54, 6483–6487.
27. A. D. Garg, D. V. Krysko, P. Vandenabeele and P. Agostinis, Hypericin-based photodynamic therapy induces surface exposure of damage-associated molecular patterns like HSP70 and calreticulin, *Cancer Immunol. Immunother*., 2012, 61, 215–221.
28. L. Apetoh, F. Ghiringhelli, A. Tesniere, M. Obeid, C. Ortiz, A. Criollo, G. Mignot, M. C. Maiuri, E. Ullrich, P. Saulnier, Yang, S. Amigorena, B. Ryffel, F. J. Barrat, P. Saftig, F. Levi, R. Lidereau, C. Nogues, J.-P. Mira, A. Chompret, V. Joulin, F. Clavel-

Chapelon, J. Bourhis, F. André, S. Delaloge, T. Tursz, G. Kroemer and L. Zitvogel, Toll-like receptor 4-dependent contribution of the immune system to anticancer chemotherapy and radiotherapy, *Nat. Med.*, 2007, 13, 1050–1059.
29. L. Apetoh, A. Tesniere, F. Ghiringhelli, G. Kroemer and L. Zitvogel, Molecular interactions between dying tumor cells and the innate immune system determine the efficacy of conventional anticancer therapies, *Cancer Res.*, 2008, 68, 4026–4030.
30. M. Michaud, I. Martins, A. Q. Sukkurwala, S. Adjemian, Y. Ma, P. Pellegatti, S. Shen, O. Kepp, M. Scoazec, G. Mignot, S. Rello-Varona, M. Tailler, L. Menger, E. Vacchelli, L. Galluzzi, F. Ghiringhelli, F. di Virgilio, L. Zitvogel and G. Kroemer, Autophagy-dependent anticancer immune responses induced by chemotherapeutic agents in mice, *Science*, 2011, 334, 1573–1577.
31. I. Martins, Y. Wang, M. Michaud, Y. Ma, A. Q. Sukkurwala. S. Shen, O. Kepp, D. Métivier, L. Galluzzi, J. L. Perfettini, L. Zitvogel and G. Kroemer, Molecular mechanisms of ATP secretion during immunogenic cell death, *Cell Death Differ.*, 2014, 21, 79–91.
32. I Martins, Y. Wang, M. Michaud, Y. Ma, A. Q. Sukkurwala, S. Shen, O. Kepp, D. Métivier, L. Galluzzi, J. L. Perfettini, L. Zitvogel and G. Kroemer, Molecular mechanisms of ATP secretion during immunogenic cell death, *Cell Death Differ.*, 2014, 21, 79–91.
33. M. Michaud, I. Martins, A. Q. Sukkurwala, S. Adjemian,Y. Ma, P. Pellegatti, S. Shen, O. Kepp, M. Scoazec, G. Mignot, S.Rello-Varona, M. Tailler, L. Menger, E. Vacchelli, L. Galluzzi, F. Ghiringhelli, F. di Virgilio, L. Zitvogel and G. Kroemer, Autophagy-dependent anticancer immune responses Induced by chemotherapeutic agents in mice, *Science*, 2011, 334, 1573–1577.
34. J. Pol, E. Vacchelli, F. Aranda, F. Castoldi, A. Eggermont, G. Cremer, C. Sautès-Fridman, J. Fucikova, J. Galon, R. Spisek, E. Tartour, L. Zitvogel, G. Kroemer and L. Galluzzi, Trial Watch: Immunogenic cell death inducers for anticancer chemotherapy, *OncoImmunology*, 2015, 4, e1008866.
35. M. Dudek, A. D. Garg, D. V. Krysko, D. De Ruysscher and P. Agostinis, Inducers of immunogenic cancer cell death, *Cytokine Growth Factor Rev.*, 2013, 24, 319–333.
36. X. Xu, K. Araki, S. Li, J.-H. Han, L. Ye, W. G. Tan, B. T. Konieczny, M. W. Bruinsma, J. Martinez, E. L. Pearce, D. R. Green, D. P. Jones, H. W. Virgin and R. Ahmed, Autophagy is essential for effector CD8+ T cell survival and memory formation, *Nat. Immunol.*, 2014, 15, 1152–1161.
37. L. Galluzzi, J. M. Bravo-San Pedro, S. Demaria, S. C. Formenti and G. Kroemer, Activating autophagy to potentiate immunogenic chemotherapy and radiation therapy, *Nat. Rev. Clin. Oncol.*, 2017, 14, 247–258.
38. M. Mauthe, I. Orhon, C. Rocchi, X. Zhou, M. Luhr, K.-J. Hijlkema, R. P. Coppes, N. Engedal, M. Mari and F. Reggiori, Chloroquine inhibits autophagic flux by decreasing autophagosome-lysosome fusion, *Autophagy*, 2018, 14, 1435–1455.
39. A. D. Garg, S. Elsen, D. V. Krysko, P. Vandenabeele, P. de Witte and P. Agostinis, Resistance to anticancer vaccination effect is controlled by a cancer cell-autonomous phenotype that disrupts immunogenic phagocytic removal, *Oncotarget*, 2015, 6, 29.
40. L. Zitvogel, O. Kepp, L. Senovilla, L. Menger, N. Chaput and G. Kroemer, Immunogenic tumor cell death for optimal anticancer therapy: The calreticulin exposure pathway, *Clin. Cancer Res.*, 2010, 16, 3100–3104.

41. B. Englinger, C. Pirker, P. Heffeter, A. Terenzi, C. R. Kowol, B. K. Keppler and W. Berger, Metal drugs and the anticancer immune response, *Chem. Rev*., 2019, 119, 1519– 1624.
42. Y.-J. Wang, R. Fletcher, J. Yu and L. Zhang, Immunogenic effects of chemotherapy-induced tumor cell death, *Genes Dis*., 2018, 5, 194–203.
43. C. A. Wootton, C. Sanchez-Cano, A. F. Lopez-Clavijo, E. Shaili, M. P. Barrow, P. J. Sadler and P. B. O'Connor, Sequence-dependent attack on peptides by photoactivated platinum anticancer complexes, *Chem. Sci.*, 2018, 9, 2733– 2739.
44. J. Du, Y. Wei, Y. Zhao, F. Xu, Y. Wang, W. Zheng, Q. Luo, M. Wang and F. Wang, A photoactive platinum(IV) anticancer complex inhibits thioredoxin–thioredoxin reductase system activity by induced oxidization of the protein, *Inorg. Chem*., 2018, 57, 5575–5584
45. A. L. Harris, Hypoxia—a key regulatory factor in tumour growth, *Nat. Rev. Cancer*, 2002, 2, 38–47.
46. S. Monro, K. L. Colón, H. Yin, J. Roque, P. Konda, S. Gujar, P.Thummel, L. Lilge, C.G. Cameron and S. A. McFarland, Transition metal complexes and photo-dynamic therapy from a tumor-centered approach: Challenges, opportunities, and highlights from the development of TLD1433, *Chem. Rev.*, 2019, 119, 797–828.